Preparation and Characterization of Composite Polymer Electrolytes Based on UV-Curable Vinylic Ether-Containing Cyclotriphosphazene, $LiClO_4$, and α-Al_2O_3

Y. W. Chen-Yang,*,† S. Y. Chen,† C. Y. Yuan,† C. H. Tsai,† and D. P. Yan‡

Department of Chemistry and Center for Nanotechnology, Chung Yuan Christian University, Chung-Li 32023, Taiwan, Republic of China, and Department of Chemistry, Chung Shan Institute of Science and Technology, Taoyuan 320, Taiwan, Republic of China

Received May 3, 2004; Revised Manuscript Received January 8, 2005

ABSTRACT: A new UV-curable vinylic ether-containing cosubstituted cyclotriphosphazene, $N_3P_3(O(CH_2CH_2O)_2CH_3)_3(OCH_2CH_2OCH{=}CH_2)_3$, [$V_3M_3$], was synthesized with high yield. This cosubstituted cyclotriphosphazene was characterized by FT-IR, ESI-MS, and ^1H,^{13}C, and ^{31}P NMR spectroscopy. A series of free-standing films with thickness of about 200 μm of V_3M_3-based composite polymer electrolytes were then prepared by mixing V_3M_3 with various amounts of $LiClO_4$ salt and α-Al_2O_3 and cured by UV irradiation. The cation−oxygen interactions in the cured polymer electrolytes were investigated by FT-IR spectroscopy. The ionic conductivities of the cured polymeric membranes measured by ac impedance measurements showed that the best conductivity of the as-prepared solid polymer electrolyte film at room temperature was 3.5×10^{-5} S/cm. The result of the cyclic voltammetry measurements revealed that the V_3M_3-based composite polymer electrolyte films were electrochemically stable up to about 4.2 V.

Introduction

The extreme fast technological progress in portable telecommunications and electronics industries such as cellular phones, personal computers, notebook computers, and camcorders requires lighter, slimmer, and safer energy sources. Thus, the thrust of scientific research is directed for technological incentives to the development of more effective and efficient ways of converting and storing a large amount of energy in a small package, light in weight and safe to use. A lithium polymer battery is the most promising way of delivering such performance needs as well as high energy density, ability to be leak-proof, lack of environmental pollution, and broad electrochemical stability.[1−5] Lithium polymer batteries use ionically conducting electrolytes instead of conventional insulating separators. The main advantages of polymeric electrolytes are favorable mechanical properties, ease of fabrication of thin films of desirable sizes, and the ability to form effective electrolyte−electrode contacts. Gel polymer electrolytes are considered as promising candidates for high-energy electrochemical devices. A large group of research has been directed toward the improvement of ambient temperature conductivity of polymer electrolytes.[6−9] Gel-type polymer films usually give good ionic conductivity, but other properties such as processability, mechanical strength, electrochemical stability window, and the Li/electrolyte interface are also key factors, especially in terms of manufacturability as well as battery reliability and recharge ability.[10]

Cross-linking is an alternative approach to provide mechanical strength to polymer electrolytes, and it provides anchoring points for the chains and, therefore, these links retain excessive movement of polymer segments. The cross-linked polymer electrolytes exhibited fully amorphous features and showed favorable ionic conductivity at an ambient temperature.[11]

The γ-radiation and chemically induced cross-linking reaction methods were applied to poly[bis(2-(2′-methoxyethoxy)ethoxy)phosphazene] (MEEP) polymer electrolytes[12] and gel electrolytes.[13] The cosubstituent polyphosphazene of (methoxyethoxy)ethoxy and poly(ethylene glycol)methyl ether has been reported.[14] Conductivity studies on composite polymer electrolytes based on MEEP were reported in our earlier work.[15] The polyphosphazene bearing branched oligoethylene side groups showed higher dimensional stabilities than MEEP.[16] Nevertheless, the most fully developed and commercially feasible route to synthesize poly(dichlorophosphazene) is use of the thermal ring-opening polymerization of hexachlorocyclotriphosphazene, $(N{=}PCl_2)_3$, at 250 °C, which yields poly(dichlorophosphazene) $(N{=}PCl_2)_n$, but with little or no molecular weight control and with large polydispersities.[7,17] To avoid the shortcoming, in this study, a new UV-curable vinylic ether-containing cosubstituted cyclotriphosphazene (V_3M_3) was synthesized and cured in the presence of $LiClO_4$ and/or α-Al_2O_3 to form the corresponding polymer electrolytes. The ionic conductivity, thermal stability, and electrochemical properties of the as-prepared V_3M_3-based polymer electrolytes were investigated.

Experimental Section

Materials. Hexachlorocyclotriphosphazene ($N_3P_3Cl_6$) (Strem Chemical Com.) was purified by recrystallization from hexane and dried in a vacuum-drying oven. Diethylene glycol monomethyl ether (Tedia Co.) and ethylene glycol vinyl ether (Aldrich Com.) were dried over 4 Å molecular sieves before use. Lithium perchlorate (Acros Com.) and α-Al_2O_3 (Aldrich Com., particle size 1 μm) were used after drying under reduced pressure at 140 °C for 24 h. Tetrahydrofuran (THF) (Merck Com.) was distilled into the reaction flask from sodium benzophenone ketyl under an atmosphere of dry nitrogen prior to use. Dichloromethane (Merck Com.) was dried and distilled from CaH_2. Other chemicals and reagents such as dichloromethane (Aldrich Com.), magnesium sulfate anhydrous

† Chung Yuan Christian University.
‡ Chung Shan Institute of Science and Technology.
* Corresponding author.

10.1021/ma049139a CCC: $30.25
Published on Web 02/26/2005

(Merck Com.), benzophenone (BPO) (Lancaster Com.), and sodium hydride (Acros Com.) were used as received. The reactions were carried out under an atmosphere of dry nitrogen.

Synthesis of Monomer. To synthesize the monomer tri(vinylicethoxyethoxy)tri(methoxyethoxyethoxy)cyclotriphosphazene (V_3M_3), (methoxyethoxyethoxy)trichlorocyclotriphosphazene (M_3C_3) was synthesized first as in the following. Hexachlorocyclotriphosphazene (20.0 g, 0.058 mol) was dissolved in 200 mL of THF. Diethylene glycol monomethyl ether (22.8 g, 0.190 mol) was added to a suspension of 60% NaH (7.72 g, 0.193 mol) in 200 mL of THF to form a sodium alkoxide solution and then added dropwise to the stirred solution of hexachlorocyclotriphosphazene at −78 °C. The reaction mixture was allowed to warm to room temperature and was monitored by ^{31}P NMR spectrometry. When the ^{31}P NMR spectrum showed the disappearance of the disubstituted product (δ (ppm): 19.1 (d, 2P), 25.4 (t, 1P)) and the formation of tris-substituted species was confirmed in situ by the singlet at 22.1 ppm, the solvent was removed by rotary evaporation, and the resultant oil was dissolved in 50 mL of dichloromethane and 50 mL of distilled water. The organic layer was collected and dried over anhydrous $MgSO_4$. The solvent was then removed by rotary evaporation. Chromatography eluting with ethyl acetate−methanol (9:1 v/v) was performed to separate the desired product. Similar fractions were combined to yield a pale yellow oil, $N_3P_3(OCH_2CH_2OCH_2CH_2OCH_3)_3Cl_3$, M_3C_3 (24.0 g, 69.2% yield). ^{1}H NMR ($CDCl_3$): δ (ppm) 3.33 (s, 9H), 3.51 (t, 6H), 3.55 (t, 6H), 3.62 (t, 6H), 3.70 (t, 6H). ^{31}P NMR ($CDCl_3$): δ (ppm) 22.1 (trans, 90%), 22.3 (cis, 10%).

Then, ethylene glycol vinyl ether (17.7 g, 0.201 mol) was added to a suspension of 60% NaH (8.28 g, 0.207 mol) in 500 mL of THF and refluxed for 24 h. The resultant sodium salt solution was added dropwise to a stirred solution containing 34.5 g of M_3C_3 in 100 mL of THF. This reaction mixture was monitored by ^{31}P NMR over 2 days and then refluxed for 24 h to make sure the reaction was complete. The product solution was purified first by removing most of the NaCl produced by centrifuge and eliminating THF by rotary evaporation. Then the residue was dissolved in 50 mL of dichloromethane and 50 mL of distilled water. While the organic phase was separated from the water phase, we collected the organic layer and added some anhydrous $MgSO_4$ to absorb the remaining water. The solvent was then removed by rotary evaporation. The product was a pale yellow oil (36.4 g, 84.1% yield).^{1}H NMR ($CDCl_3$): δ (ppm) 3.58 (s, 9H), 3.72 (t, 6H), 3.83 (t, 6H), 3.88 (t, 6H), 4.05 (t, 6H), 4.17 (dd, 3H), 4.23 (t, 6H), 4.30 (t, 6H), 4.34 (dd, 3H), 6.46 (dd, 3H). ^{13}C NMR ($CDCl_3$): δ (ppm) 59.0, 64.0, 65.0, 66.7, 70.0, 70.5, 71.9, 86.8, 151.5. ^{31}P NMR ($CDCl_3$): δ (ppm) 18.4 (s, 3P). IR (film): 1231 (P=N), 2926, 1457 (C−H), 1457, 989 (P−O−C), 1058, 1110 (C−O−C), 1620 (C=C). ESI: $MH^+ = 754.3$.

Preparation of Composite Solid Polymer Electrolytes. Appropriate amounts of lithium perchlorate ($LiClO_4$), α-aluminum oxide (α-Al_2O_3), and the photoinitiator (BPO) were mixed with V_3M_3 in 2.0 mL of THF for 12 h to prepare a homogeneous electrolyte solution. The solution was cast on a Teflon plate, vacuum-evaporated for 1 h at 60 °C to remove the solvent, and irradiated by UV (365 nm) for 3 h to prepare the cross-linked polymer electrolyte films. The thickness of the polymer electrolyte films was about 200 μm.

Instruments. ^{1}H, ^{13}C, and ^{31}P NMR spectra were recorded with a Bruker AC-300 NMR spectrometer operating at 300.13, 75.47, and 121.49 MHz, respectively. The ^{13}C NMR spectra were proton-decoupled, and the chemical shifts were referenced to an internal $CDCl_3$ sample. ^{31}P NMR chemical shifts were relative to 85% phosphoric acid as an external reference, with positive shift values downfield from the reference. The ionic conductivities of the polymer electrolytes were measured by the complex impedance method in the temperature range from 30 to 80 °C. The samples were sandwiched between stainless steel blocking electrodes and placed in a temperature-controlled oven at vacuum ($<10^{-2}$ Torr) for 2 h before measurement. The ac impedance measurements were carried out on a computer-interfaced HP 4192A impedance analyzer over the frequency range 5 Hz−13 MHz. The FTIR spectra were recorded on a Bio-Rad FTS-7 system with a wavenumber resolution of 2 cm^{-1} in the range of 400−4000 cm^{-1} (film). The DSC and TGA measurements were performed with a Seiko DSC 200C and a Seiko TG/DTA 220, respectively. A linear sweep voltammetry (LSV) experiment was carried out on the Li/solid polymer electrolytes/SS cell at scanning rate of 10 mV/s to measure the electrochemical stability window.

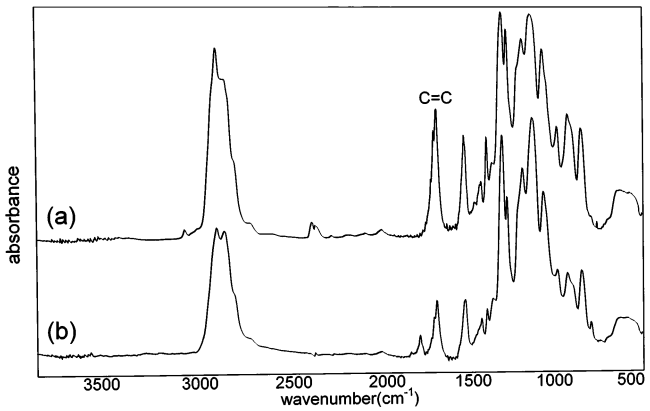

Figure 1. FT-IR spectra of (a) V_3M_3 and (b) cured V_3M_3.

Scheme 1

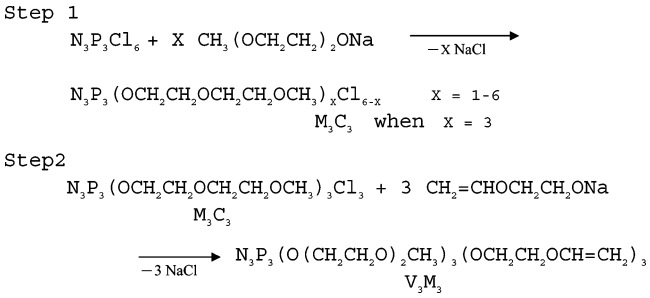

Results and Discussion

Synthesis of V_3M_3 Cyclotriphosphazene. The synthesis of V_3M_3 was carried out according to Scheme 1. In the first step, M_3C_3 was synthesized by reacting hexachlorocyclotriphosphazene with sodium alkoxide solution of diethylene glycol monomethyl ether. In the second step, M_3C_3 was reacted with sodium alkoxide solution of ethylene glycol vinyl ether to form V_3M_3.

The identity and purity of the UV-curable monomer tri(vinylicethoxyethoxy)tri(methoxyethoxyethoxy)-cyclotriphosphazene (V_3M_3) were characterized and confirmed by ^{1}H, ^{13}C, and ^{31}P NMR, ESI-MS, and FT-IR spectroscopies as indicated in the Experimental Section. The ^{31}P NMR spectrum of V_3M_3 showed a singlet peak. The chlorine atoms on phosphazene ring were completely displaced by two different kinds of alkyloxy groups; however, no distinctive P-shift was observed, which might be attributed to the fact that $P(OR)_2$ and P(OR)(OR′) were nearly isochronous. The ^{1}H NMR integral ratio of the peak area for OCH_3 versus OCH = (approximately 3:1) together with the ESI-mass spectrometry analysis ($MH^+ = 754.3$) further confirmed the composition of V_3M_3 to be $N_3P_3(O(CH_2CH_2O)_2CH_3)_3(OCH_2CH_2OCH{=}CH_2)_3$.

UV-Curing of V_3M_3. The chemical structures of V_3M_3 and the UV-cured polymer networks with and without the salt were compared by examining the FT-IR spectra. As shown in Figure 1a, for V_3M_3, the peaks for the P=N stretching of the cyclic ring are found in the region of 1200−1230 cm^{-1}. The absorption frequen-

Table 1. Conductivities and T_g of the Solid Polymer Electrolytes (SPE) Based on Cured $V_3M_3/LiClO_4$ at 30 °C

sample	[O]/[Li][a]	conductivities (S/cm)	T_g (°C)
SPE-1	30	2.6×10^{-6}	−50.2
SPE-2	20	8.7×10^{-6}	−48.4
SPE-3	15	1.5×10^{-5}	−43.9
SPE-4	12	1.8×10^{-5}	−44.6
SPE-5	10	2.1×10^{-5}	−46.4
SPE-6	8	1.9×10^{-5}	−43.5
SPE-7	6	5.9×10^{-6}	−43.1

[a] The molar ratio of the ethylene oxygen and the lithium salt.

cies for P−O−C and C−O−C stretches of the methoxyethoxyethoxy (MEE) side chain groups are appearing at 890−990 and 1090−1110 cm^{-1}, respectively. The C═C stretching of the vinylic ether group is found at 1620 cm^{-1}. These absorption peaks confirm the structure of M_3V_3, as expected. After UV-curing it is observed that the intensity of the C═C stretching peak at 1620 cm^{-1} is decreased, indicating that the polymer obtained was partially cured through the C═C bonds. Besides, it was found that for shorter exposure of UV curing the ionic conductivity values were higher, but the electrolyte films were sticky material with poor mechanical stability as compared with long time exposure of UV. In addition to high conductivity values, to obtain mechanically stronger species, the UV-curing time for the present work was fixed at 3 h.

Conductivity Studies. The ionic conductivities of the as-prepared electrolytes were obtained by the ac impedance analysis as described previously.[18] The conductivity values obtained for the cured $V_3M_3/LiClO_4$ solid polymer electrolyte (SPE-X) films as a function of salt concentration are summarized in Table 1. It is found that for the electrolyte system with [O]/[Li] = 30−10, molar ratio of the ethylene oxide concentration to the lithium salt, the ionic conductivity is increased with increasing Li salt content. However, the ionic conductivity decreases for concentrations [O]/[Li] ≥ 8. The ionic conductivity of a polymer electrolyte depends on the actual concentration of the conducting species and their mobility. Initial increase of ionic conductivity when [O]/[Li] = 30−10 is due to the increment of the number of charge carriers being introduced into the complex. As the salt concentration increases, the effects such as ion pairs or ion triplet formation, charge cloud effects, and restriction to chain mobility cause the ionic movement to drop and thereby a reduction in ionic conductivity value. Thus, the ionic conductivity data pass through the maximum value for [O]/[Li] = 10 and thereafter decrease as the molar concentration of salt increases. Similar observations are also reported by Kim et al.[19,20] So the concentration of lithium salt was fixed to this value for the rest of the study. The conductivity value (2.1×10^{-5} S/cm) of the SPE-5 standing film is comparable with the values reported by Abraham et al.[17] for the MEEP-based polymer electrolyte.

On the other hand, much of the recent research efforts to improve the ambient temperature conductivity while retaining the mechanical properties and the stability toward metallic lithium anode have been directed toward the addition of ultrafine particles of ceramic fillers such as Al_2O_3, SiO_2, and TiO_2 for polymer electrolytes to obtain composite polymer electrolytes. Experimental evidence from various groups consistently show that the ionic conductivity was improved over a wide temperature range, the interface between lithium and a composite electrolyte was more stable and

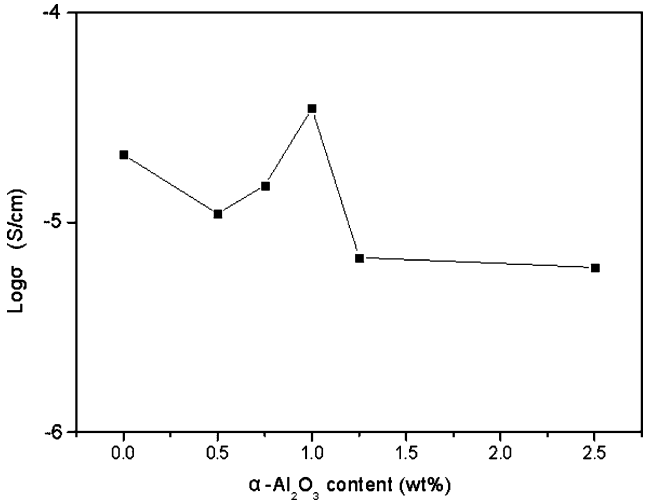

Figure 2. Change in conductivity of the cured V_3M_3-based composite polymer electrolytes CPE with different filler (α-Al_2O_3) content at 30 °C ([O]/[Li] = 10).

Table 2. Arrhenius Parameters and T_g of the CPEs with Various α-Al_2O_3 Content ([O]/[Li] = 10)

sample	α-Al_2O_3 content (wt %)	E_a (kJ/mol)	σ (S/cm^{-1}) 30 °C	σ (S/cm^{-1}) 80 °C	T_g (°C)
SPE-5	0	16.7	2.1×10^{-5}	3.1×10^{-4}	−46.4
CPE-1	0.5	18.4	1.1×10^{-5}	5.5×10^{-5}	−38.4
CPE-2	0.75	17.8	1.5×10^{-5}	1.5×10^{-4}	−40.3
CPE-3	1.0	15.8	3.5×10^{-5}	5.7×10^{-4}	−42.0
CPE-4	1.25	18.1	6.8×10^{-6}	5.3×10^{-5}	−33.5

efficient in cycling, and the Li ion transport number was enhanced in comparison to the filler-free electrolyte.[15,23−27] Figure 2 presents the variation of ionic conductivity of the cured V_3M_3-based composite polymer electrolytes (CPE-X) as a function of α-Al_2O_3 concentration. As noticed, the ionic conductivity was first decreased when 0.5 wt % of α-Al_2O_3 was added and then increased when more of filler was dispersed in, yet it decreased again when the filler content was larger than 1.0 wt %. It is found that the conductivity increases with α-Al_2O_3 concentration and showed a maximum value of 3.5×10^{-5} S/cm, corresponding to a sample with 1.0 wt % of α-Al_2O_3, beyond which it demonstrates the inverse effect. This result may be reasoned as follows. For the electrolyte with trace amount of α-Al_2O_3, the nanoparticle fillers were well dispersed in the polymer chains, leading to the formation of the strong polymer chain−filler interaction. For the electrolyte with medium content of α-Al_2O_3, the filler not only had interaction with the polymer chain but also provided the "ion hopping sites" assisting lithium cation to migrate in the system. From Table 2 it can also be seen that the composite containing 1.0 wt % of α-Al_2O_3 shows the lowest activation energy, confirming that the Li^+ ion has a higher mobility in the system due to the optimal effect caused by the filler which provided the hopping sites and transient-cross-linking to the polymer, which provides coordinating oxygen atoms. For higher filler concentration, the blocking effect or the geometrical constrictions imposed by the more abundant alumina grains could make the long polymer chain more "immobilized", leading to lower conductivity. So the addition of optimum concentration of fillers act as cross-linking centers for polymer segments to create highly conductive pathways along the filler surface, inducing an increase in conductivity. A reduction in the glass transition

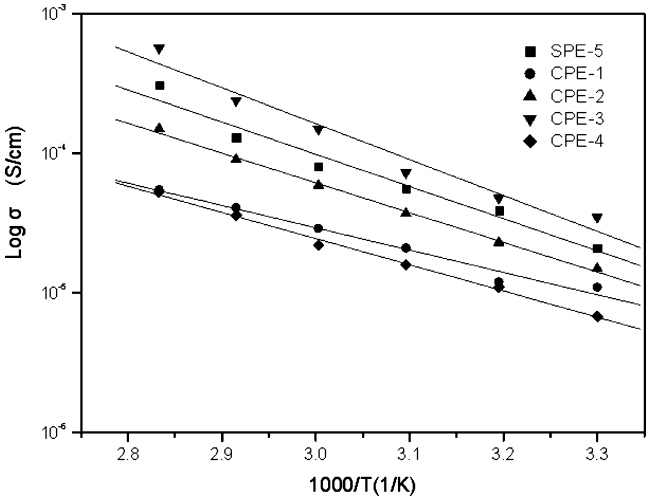

Figure 3. Arrhenius plots of the ionic conductivity of the CPEs with different α-Al_2O_3 content.

temperature (T_g) of the polymer electrolyte for the addition of 1.0 wt % of α-Al_2O_3 when compared to other filler concentrations (Table 2) was also observed. Similar behavior was reported for the MEEP-based[15] and PAN-based[25] polymer electrolytes. The above observation can also be explained by the ideas proposed by Mellandar et al.[26] regarding the role played by the alumina fillers in composite polymer electrolytes. According to their ideas, Lewis acid−base type oxygen and O−H surface groups on alumina grains interact with cations and anions and provide additional sites creating favorable high conducting pathways in the vicinity of grains for the migration of ions.

The temperature dependence of electrical conductivities of the polymer films is shown in Figure 3. It shows that all the ionic conductivity was linearly increased with increasing temperature. The linear plots indicate that the ionic conductivity data of all the α-Al_2O_3-containing composite polymer electrolytes follow the Arrhenius equation

$$\sigma(T) = \sigma_0 \exp\{-E_a/RT\}$$

where σ_0 is the conductivity preexponential factor and E_a is the activation energy for the ion conductivity. The activation energies calculated from the linear slopes of the Arrhenius plots (Figure 3) are in the range $E_a \doteqdot$ 15.8−18.4 kJ/mol. The composite polymer electrolyte containing 1 wt % of α-Al_2O_3 possess a minimum value of activation energy (15.8 kJ/mol). This value is low in comparison with E_a values of thermoplastic polyurethane (TPU)−PAN (18.2 kJ/mol) composite electrolyte,[27] implying a better environment for ion conduction in this composite electrolyte.

FT-IR Studies. The FTIR spectra of polymer electrolytes vary according to their compositions and may be able to show the occurrence of the complexation and interaction between the various constituents. In the present work, the changes in the FT-IR spectra shown in Figure 4 could be ascribed to the interactions between Li^+ ion and the lone pair electrons of the ether oxygen on the polymer side chains. If the alkali metal cations are coordinated to the ether oxygen of the side chains, then one would expect a negative shift in the wavenumber of the C−O−C and P−O−C stretching regions.[28] In the present work, the absorption peaks at 1109 and 983 cm^{-1} are shifted to the values of 1090 and 980 cm^{-1},

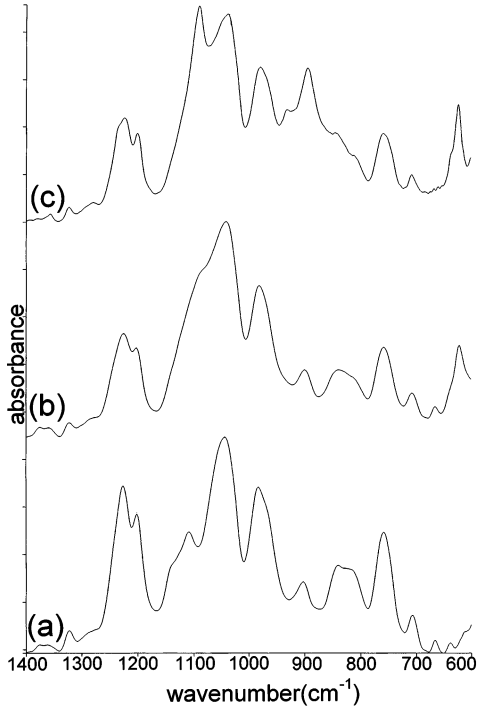

Figure 4. FT-IR data of (a) cured V_3M_3, (b) SPE-5, and (c) CPE-1.

respectively, in the complex. This downshift in wavenumber of the C−O−C stretching mode corresponds to a weaker ion−polymer interaction that provides more free Li^+ for improved ionic transport. For the addition of α-Al_2O_3 particles to CV_3M_3 polymer electrolytes, the shape of the C−O−C stretching mode is changed into two new bands appearing at 1039 and 1090 cm^{-1}. These two newly formed bands can be attributed to the cation−anion interaction.[29] The absorption band at about 938 cm^{-1} is assigned to the totally symmetric vibrations of perchlorate anions.[28] The frequency of this band is sensitive to ion association. Since the polarizing effect of the counterion in an ion pair or a multiple ion aggregate leads to an upshift of the frequency as compared with the unperturbed anion, it is unable to be investigated in this present study because the absorbance is overlapped with that of P−O−C vibration of phosphazene.

The ν_4 stretch of ClO_4^- is resolved into two contributions at 621 and 639 cm^{-1} in the polymer complex. The peak appearing at 621 cm^{-1} is attributed to the spectroscopically "free" ClO_4^- anion and the other at 639 cm^{-1} associated with the bound ClO_4^- anion.[15] When α-Al_2O_3 added to this as-prepared polymer electrolyte, the peak appearing at 639 cm^{-1} disappeared, and the other peak shifted to 623 cm^{-1} with increased intensity. The decrease of the area under the 639 cm^{-1} mode corresponds to a decrease in ion association accompanied by an increase in conductivity.[30]

For the uncomplexed cured polymer (CV_3M_3), the C−H stretching frequency is measured at 841 cm^{-1}; it decreases to 831 cm^{-1} after $LiClO_4$ is complexed. As the volume fraction of the filler is increased, it disappears; i.e., the addition of α-Al_2O_3 reduces the interaction between the ether oxygen of CV_3M_3 and Li^+ cations. In other words, part of the interaction is disrupted due to the presence of the dispersed α-Al_2O_3 particles. Here, the changes are connected with the role of the coordination of the Li^+ cation. These coordinations are made in

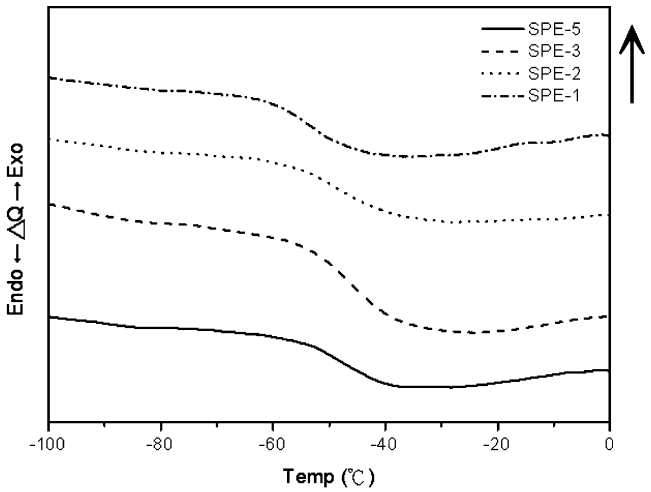

Figure 5. DSC thermograms of the SPEs with various amounts of $LiClO_4$.

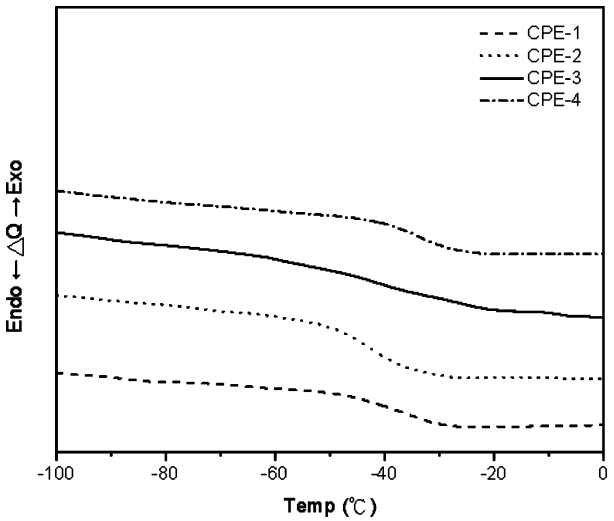

Figure 6. DSC thermograms of the CPEs with various amounts of α-Al_2O_3.

such a way as to increase the flexibility of the polymer segments.[29] The appearance of new peaks along with changes in the existing peak in the FTIR spectra confirms the complexation.

Thermal Studies. Since the solid polymer electrolyte films were prepared by photoinduced radical polymerization of V_3M_3, the as-prepared electrolytes were expected to have 3-dimensional network structures. The DSC thermograms shown in Figure 5 elucidate the effect of $LiClO_4$ on the thermal transition of the cured polymer. It is seen that T_g was increased with the increase of the $LiClO_4$ content. The increase of T_g (as listed in Table 1), indicating the retardation of the motion of the polymer matrix, implies the existence of the interaction between Li^+ ions and the atoms containing lone pair electrons. The DSC traces of the α-Al_2O_3 added polymer electrolyte samples are displayed in Figure 6. It is seen that the T_g is further increased with increasing α-Al_2O_3 content, indicating the formation of the transient cross-linking effect caused by the α-Al_2O_3 particles. When ceramic fillers are finely dispersed in the matrix, the tremendous surface area developed could contribute to polymer chain confinement effects that may lead to higher glass transition temperature, stiffness, and strength.[31]

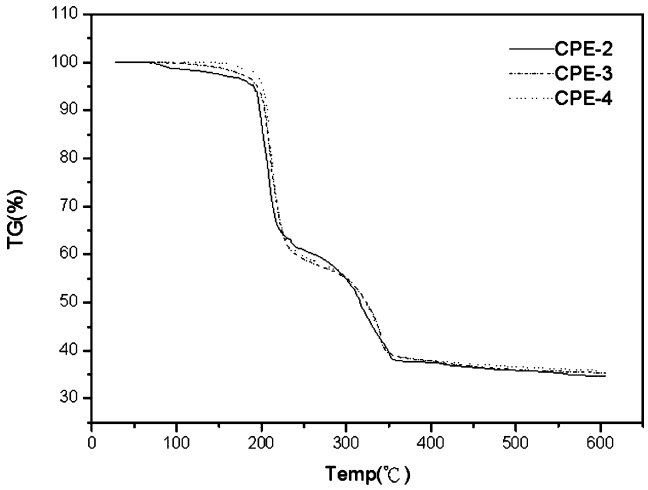

Figure 7. TGA thermograms of the CPEs with various amounts of α-Al_2O_3.

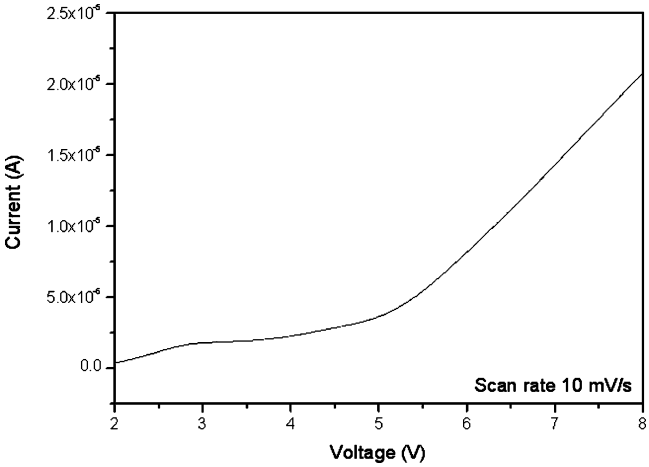

Figure 8. Linear sweep voltammetry for CPE-3 at 30 °C.

Figure 7 shows the TGA thermograms for the cured V_3M_3-based composite polymer electrolytes. As noticed, the thermal decomposition of the composite electrolytes were proceeded by a two-step process: (1) the decomposition of the etheric side chains connecting to the phosphazene ring at 211 °C and (2) the decomposition of the backbone P=N bond at 343 °C. Furthermore, $T_{5\%}$, the temperature at which 5% weight was lost, was above 180 °C and slightly increases with increasing α-Al_2O_3 content, indicating that the thermal stability of the electrolyte was enhanced slightly due to the presence of the α-Al_2O_3 nanoparticles. Thus, these composite polymer electrolyte films were stable up to 180 °C, which was higher than the operating temperature of the lithium polymer cell (50−70 °C).

Electrochemical Stability Window. One of the important parameters in the characterization of polymer electrolytes is the electrochemical stability window, especially in view of applications for lithium batteries. The electrochemical stability of CPE-3 was studied as an example by means of linear sweep voltammetry of a symmetric cell type Li/CPE/SS where lithium was used as the counter electrode. Figure 8 shows the linear sweep voltammogram of the Li/CPE-3/SS cell at a scanning rate of 10 mV/s. The voltage was swept from the open-circuit voltage of the cell toward more positive voltage values until a great current charge due to electrolytes decomposition at the inert electrode interface occurred. The potential window obtained was above

4.2 V for this material, indicating that the CPE has an electrochemical stability window of at least 4.2 V, thus ensuring their use with the most common lithium-based couples, which have voltages of about 3.0−4.0 V.

Conclusion

In the present investigation, we synthesized a new UV-curable cyclic phosphazene, V_3M_3, and prepared a series of V_3M_3-based cross-linked composite solid polymer electrolytes (CPEs). The complex formation has been confirmed by FTIR studies. The experimental results indicated that the amounts of $LiClO_4$ and α-Al_2O_3 nanoparticles significantly affected the ionic conductivity of the CPE. A maximum ionic conductivity of 3.5×10^{-5} S/cm at room temperature was obtained from CPE-3. The thermal stability of the films was also examined using DSC and TGA studies. Though the conductivity values of the as-prepared CPE materials were comparable to that of MEEP, the cured V_3M_3-containing CPE films appeared to have better dimensional stability and workability than MEEP. This indicates that the cured V_3M_3-based CPE may be a potential candidate for rechargeable lithium batteries.

Acknowledgment. The authors thank the National Science Council and Chung-Shan Institute of Science Technology of Taiwan, R.O.C., for financially supporting this research under Contract NSC 91-2623-7-033-005. The authors are grateful to Dr. O. Mahendran for helpful discussions.

References and Notes

(1) Wen, Z.; Itoh, T.; Uno, T.; Kubo, M.; Yamamoto, O. *Solid State Ionics* **2003**, *160*, 141.
(2) Chandrasekhar, P. *Blockcopolymers/Polyelectrolytes/Biodegradation*; Springer-Verlag: Berlin, 1998; Vol. 135.
(3) Meyer, W. H. *Adv. Mater.* **1998**, *10*, 439.
(4) Blonsky, P. M.; Shriver, D. F.; Austin, P. E.; Allcock, H. R. *J. Am. Chem. Soc.* **1984**, *106*, 6854.
(5) Allcock, H. R.; Olmeijer, D. L.; O'Connor, S. J. M. *Macromolecules* **1998**, *31*, 753.
(6) Kim, C. S.; Oh, S. M. *J. Power Sources* **2002**, *109*, 98.
(7) Song, J. Y.; Yang, Y. Y.; Wan, C. C. *J. Power Sources* **1999**, *77*, 183.
(8) Koksbang, R.; Olsen, I. I.; Shackle, D. *Solid State Ionics* **1994**, *69*, 320.
(9) Siekierski, M.; Wieczorek, W.; Przyluski, J. *Electrochim. Acta* **1997**, *43*, 1339.
(10) Jiang, Z.; Carroll, B.; Abraham, K. M. *Electrochim. Acta* **1997**, *42*, 2667.
(11) Nishimoto, A.; Agerhera, K.; Furuya, N.; Watanable, T. *Macromolecules* **1999**, *32*, 1514.
(12) Bennett, J. L.; Dembele, A. A.; Allcock, A. R.; Heyen, B. J.; Shriver, D. F. *Chem. Mater.* **1989**, *1*, 14.
(13) Kono, M.; Kayashi, E.; Watanable, M. *J. Electrochem. Soc.* **1999**, *146*, 1626.
(14) Allcock, H. R. *Chem. Mater.* **1994**, *6*, 1476.
(15) Chen-Yang, Y. W.; Chen, H. C.; Lin, F. J.; Liao, C W.; Chen, T. L. *Solid State Ionics* **2003**, *156*, 383.
(16) Allcock, H. R.; O'Connor, S. J. M.; Olmeijer, D. L.; Napierala, M. E.; Cameron, C. G. *Macromolecules* **1996**, *29*, 7544.
(17) Abraham, K. M.; Alamgir, M.; Reynolds, R. K. *J. Electrochem. Soc.* **1989**, *136*, 3576.
(18) Chen-Yang, Y. W.; Huang, J. J.; Chang, F. H. *Macromolecules* **1997**, *30*, 3825.
(19) Kim, S. H.; Kim, Y. R.; Kim, H. S.; Choe, H. N. *Solid State Ionics* **1999**, *116*, 63.
(20) Kim, S. H.; Choi, J. K.; Bae, Y. C. *J. Appl. Polym. Sci.* **2001**, *81*, 948.
(21) Quartarone, E.; Mustarelli, P.; Magistris, A. *Solid State Ionics* **1998**, *110*, 1.
(22) Kim, Y. W.; Lee, W.; Choi, B. K. *Electrochim. Acta* **2000**, *45*, 1473.
(23) Swierczynki, D.; Zalewska, A.; Wieczorek, W. *Chem. Mater.* **2001**, *13*, 1560.
(24) Croce, F.; Apperecchi, G. B.; Persi, L.; Scrosati, B. *Nature (London)* **1998**, *394*, 456.
(25) Chen-Yang, Y. W.; Chen, H. C.; Lin, F. J. *Solid State Ionics* **2002**, *150*, 327.
(26) Dissanayalce, M. A. K. L.; Jayathilaka, P. A. R. D.; Bokalawala, R. S. P.; Albinsson, I.; Mellander, B. E. *J. Power Sources* **2003**, *119*, 409.
(27) Kuo, H. H.; Chen, W. C.; Wen, T. C.; Gopal, A. *J. Power Sources* **2002**, *110*, 27.
(28) Johanson, P.; Ratner, M. A.; Shriver, D. F. *J. Phys. Chem. B* **2001**, *105*, 9016.
(29) Wieczorek, W.; Lipka, P.; Zukowska, G.; Wycislik, H. *J. Phys. Chem. B* **1998**, *102*, 6968.
(30) Zhou, J.; Fedkiw, P. S. *Solid State Ionics* **2004**, *166*, 275.
(31) Zheng, W.; Wong, S. C.; Sue, H. J. *Polymer* **2002**, *73*, 6767.

MA049139A